JSAEM Studies in Applied Electromagnetics and Mechanics, 11

APPLICATIONS OF ELECTROMAGNETIC PHENOMENA IN ELECTRICAL AND MECHANICAL SYSTEMS

Proceedings of
The First Japanese-Australian Joint Seminar on Applications of Electromagnetic Phenomena in Electrical and Mechanical Systems
16-17 March 2000, Adelaide, Australia

Editors:

Andrew Nafalski **Mahmoud Saghafifar**
University of South Australia, Adelaide, Australia

Applications of Electromagnetic Phenomena in Electrical and Mechanical Systems
A. Nafalski and M. Saghafifar (eds)

Eddy current testing by the modified Rogowski coil

Makoto Aoki, Hisashi Endo, Seiji Hayano, Yoshifuru Saito
Graduate School of Engineering, Hosei University

ABSTRACT: This paper proposes a modified Rogowski coil to improve the precision and sensitivity of eddy current testing. This coil has been used as a current viewer that can detect the 2D current distribution with a high resolution. In the present paper, we compute the magnetic field distribution of the coil by finite element method taking into account the open boundary. As a result, it can be effectively used not only as a passive current viewer but also as an active ECT sensor.

1 INTRODUCTION

Searching for crack and defect in many equipment, such as elevators and escalators, is one of the most important applications of non-destructive testing.

In the present paper, we propose a modified Rogowski coil as a current viewer with a high resolution [1]. By means of finite element method, the magnetic field distribution caused by this coil is computed.

2 THE MODIFIED ROGOWSKI COIL

As shown in Fig.1, our proposed sensor is a curved form of a conventional solenoidal coil.

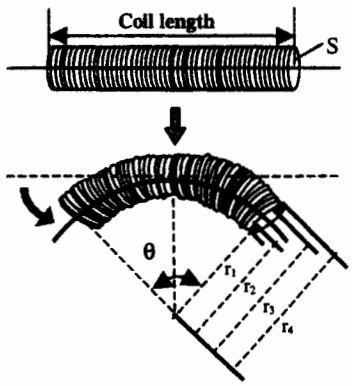

Figure 1 Schematic diagram of a conventional solenoidal coil (upper) and a modified Rogowski coil (lower).

The design parameters of our modified Rogowski coil sensor are: the cross-sectional area S, the length l, the number of turns of the conventional solenoidal coil, the radius r_1 and the angle θ.

3 THE STRATIGIC DUAL IMAGE METHOD

3.1 Principle

In most fields appearing in physical systems, the field intensity decreases on moving away from the source point. In addition, the potential may be reduced to zero, so that both the field intensity and potential become zero at an infinitely long distance from the source point. This means the symmetrical and zero boundary conditions are satisfied at infinity.

A key feature of the strategic dual image method is that any open boundary solution vector in electromagnetic field problems can be obtained by averaging the symmetrical and zero boundary solution vectors, which are respectively evaluated by imposing the symmetrical and zero boundary conditions on a hypothetical boundary located at a finite distance from the source point. Establishment of the symmetrical and zero boundary conditions at the hypothetical boundary is carried out by assuming strategic dual images.

This method is sufficient to show that the symmetrical and zero boundary solutions give the upper and lower bounds of the open boundary solution, respectively.

3.2 1D open field

Most one-dimensional electromagnetic field problems cannot be used practically, but they offer good examples to illustrate the basic idea of strategic dual image method.

In Fig.2(a), for a source electric charge Q and its image $+Q$ located at $x=2L$, a symmetrical boundary condition at $x=L$ can be established. Similarly, imposing a dual image $-Q$ at $x=L$. The average of both fields in Figs. 2(a) and (b) gives an open field caused by the source charge Q. Thus, the open boundary solution vector can be obtained by averaging the symmetrical and zero boundary solution vectors as shown in Fig.2(c).

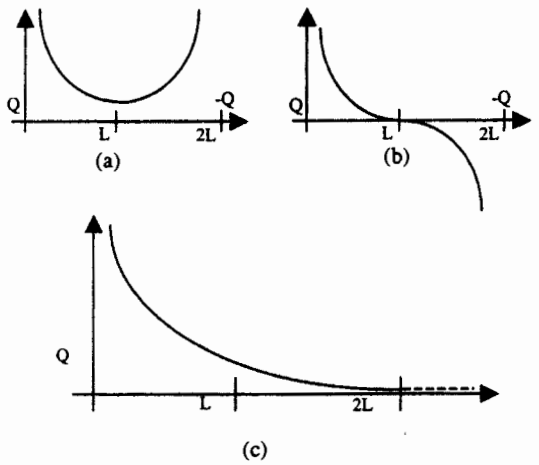

Figure 2 Strategic 1D dual images: (a) an image charge Q with a symmetrical boundary at x=L; (b) a dual image –Q with a zero boundary at x=L; (c) average of (a) and (b).

3.3 2D open field

At first, let us consider one of the currents i in the problem region. When an image current $-(d/a)i$ is imposed at the position shown in Fig.3(a) , the normal component of flux density B becomes zero at the circular hypothetical boundary. This means that the vector potential A is zero at the hypothetical boundary when the magnetic field is represented in terms of A. The zero boundary condition $A=0$ corresponds to the symmetrical boundary condition $\partial U / \partial n = 0$, when the magnetic field is represented in terms of the scalar potential U.

Secondly, let us consider one of the magnetic charges m in the problem region instead of current i. When an image $-(d/a)m$ is imposed at the position shown in Fig.2(b), the tangential component of the field intensity H becomes zero at the hypothetical boundary. This means that the scalar potential U is zero at the hypothetical boundary when the magnetic field is represented in terms of U. The zero boundary condition $U=0$ corresponds to the symmetrical boundary condition $\partial A / \partial n = 0$, when the magnetic field is represented in terms of the vector potential A.

Thus, the open 2D field solution vector can be obtained by using the circular hypothetical boundary and averaging the zero and symmetrical boundary solution vectors.

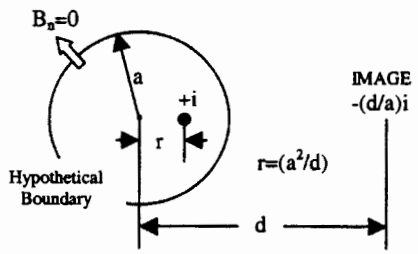

(a) the rotational field source image –(d/a) i (the zero A=0 or symmetrical $\partial U / \partial n = 0$ boundary condition established at the circular surface).

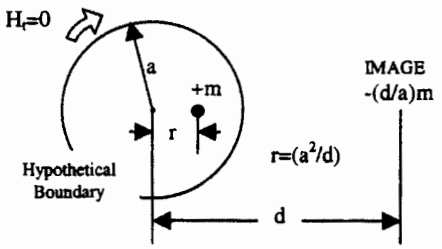

(b) the divergence field source image –(d/a) m (the zero U=0 or symmetrical $\partial A / \partial n = 0$ boundary condition established at the circular surface).

Figure 3 Strategic 2D dual image.

4 MAGNETIC FIELD ANALYSIS OF THE MODIFIED ROGOWSKI COIL

The magnetic field distributions of the modified Rogowski coil can be computed by the strategic dual image (SDI in short) method whether an iron

sheet exists in the problem region or not. Table 1 lists different constants of the tested modified Rogowski coil.

Table 1 various constants of a tested coil

r_1	r_2	r_3	r_4	Θ	Number of turn
20	29	38	47	$\pi/2$	55

Fig.4 shows the magnetic field distributions caused by the modified Rogowski coil with the problem region containing an iron sheet (a) and without iron sheet (b).

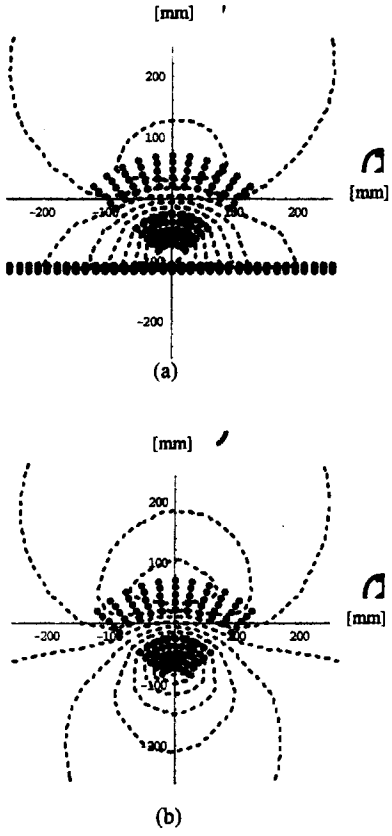

Figure 4 Magnetic field distributions by the modified Rogowski coil. (a) within iron sheet, (b) without iron sheet.

Figs.5 and 6 show the magnetic field distributions caused by a conventional solenoidal coil with the same specifications as those of the modified Rogowski coil except for the bending angle and the radius. Fig.5 shows the magnetic field distributions when the solenoidal coil is located horizontally, whereas Fig.6 shows the field distributions when the solenoidal coil is located vertically. It can be observed that the magnetic field caused by the modified Rogowski coil is concentrating to a particular point on the iron sheet locating below the sensor coil.

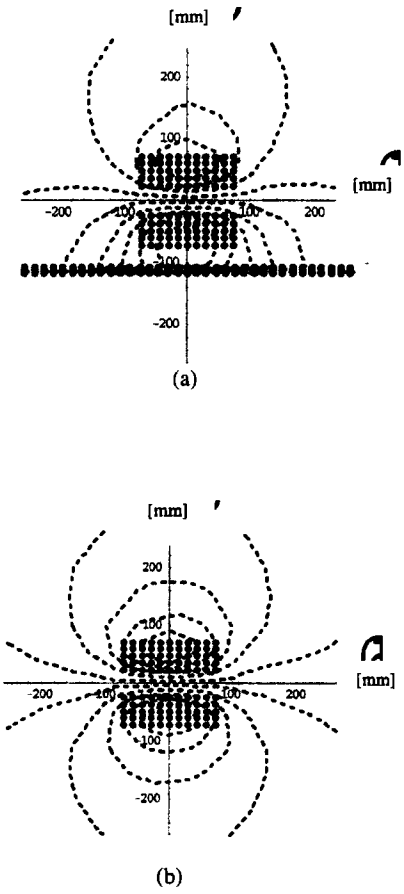

Figure 5 Magnetic field distributions caused by a solenoidal coil located horizontally (a) within an iron sheet, (b) without iron sheet.

To check the sensitivity for eddy current testing, we compared the change of inductance between the modified Rogowski and conventional coils, with and without the iron sheet in the problem region. Since each tested coil has a distinct inductance value, the inductance change was measured by a simple ratio l_i/l. Where l_i and l are the inductance values with and without the iron sheet, respectively. Table 2 lists the change of inductances. As a result, the modified Rogowski coil has an advantage over the solenoidal coil that its sensitivity does not depend on the direction.

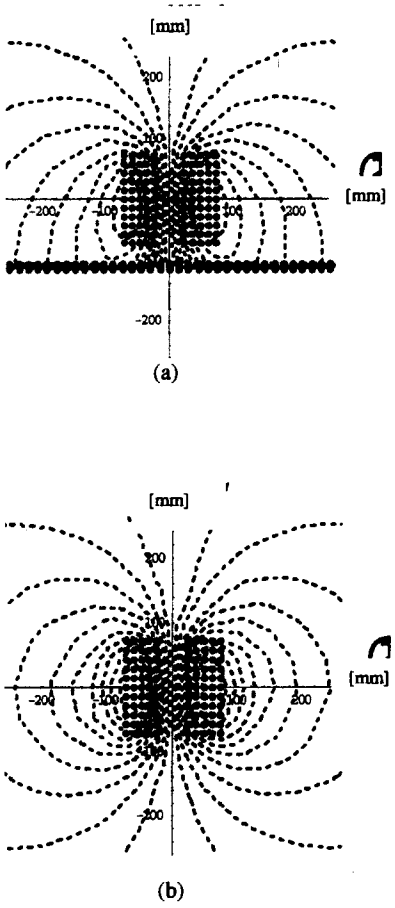

Figure 6 Magnetic field distributions caused by a solenoidal coil located vertically (a)within an iron sheet (b)without iron sheet.

Table 2 The rate of inductance changes

Modified Rogowski coil	1.14231
Solenoidal coil (Horizontal)	1.09578
Solenoidal coil (Vertical)	1.14595

5 EDDY CURRENT TESTING BY THE MODIFIED ROGOWSKI COIL

According to the SDI solutions, our modified Rogowski coil is applicable as an eddy current sensor having high sensitivity as well as high defect size resolution. Fig.7 shows a schematic diagram of the eddy current testing. In this figure, l_c denotes the length of the defect. Table 3 lists various constants of the tested modified Rogowski coil for ECT and the length l_c within a defect in an iron plate

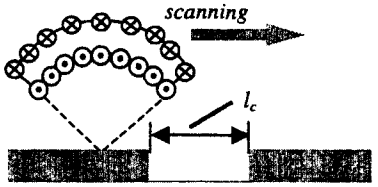

Figure 7 Schematic diagram of eddy current testing by the modified Rogowski coil.

Table 3 Various constants of the tested modified Rogowski coil for ECT and a length l_c of the defect.

r_1	r_4	θ	Number of turns	l_c
30	38	$\pi/2$	21	48

Fig.8 shows the magnetic field distributions at different sensor positions. When the sensor locates far from the defect, the major magnetic fluxes are concentrated to the iron plate below the sensor, as shown in Fig.8(a). On the other hand, when one of the edges of the sensor locates near the defect, the magnetic field distribution is dramatically changed, as shown in Fig.8(b). Furthermore, when the sensor locates just above the defect, the magnetic field distributes in a symmetrical manner, as shown in Fig.8(c).

Fig.9 shows the inductance of the modified Rogowski coil versus the sensor position with respect to the target defect. When the sensor locates in the center of the crack, the inductance reaches to a minimum. As a result, the crack is detectable using the modified Rogowski coil.

6 CONCLUSION

We have proposed a modified Rogowski coil (previously reported as a current viewer with a high resolution) to improve the applicability of eddy current testing. Using finite element method with the SDI strategy, we have computed the magnetic field distributions caused by the modified Rogowski coil taking into account the open boundary condition. As a result, it has been revealed that our modified Rogowski coil is applicable as an ECT sensor with a high position resolution.

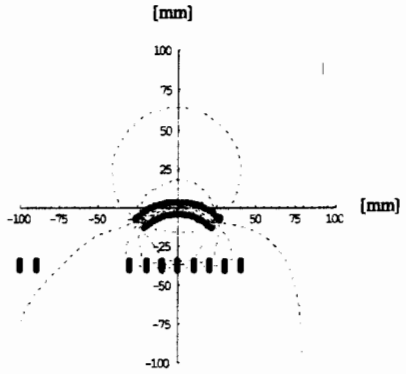

(a) Sensor locates far from the defect.

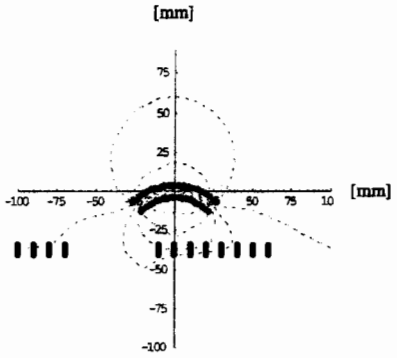

(b) one of the edges of sensor coil locates above the defect.

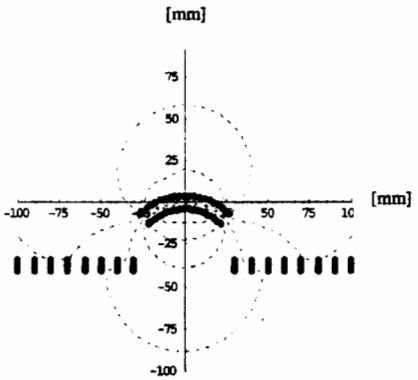

(c) sensor coil locates just above the defect.

Figure 8 Magnetic field distributions by the modified Rogowski sensor coil.

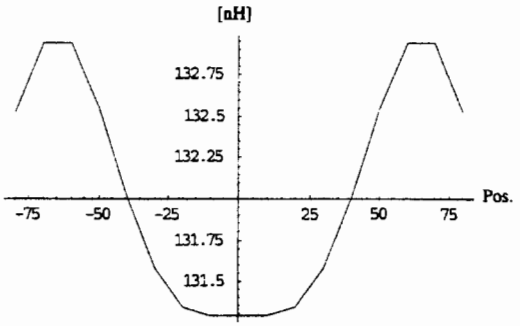

Figure 9 Variation of inductance depending on the sensor position.

7 REFERENCES

1. Aoki, M., Hayano, S., Saito, Y., Measurement of 2D Current Distribution by the Current Viewer, *Magnetic Society of IEEJ*, 1999, MAG-99-150.
2. Cortial, F., Yoshida, S., Tohya, H., Midorikawa, Y., Saito, Y., SDI (strategic Dual Image) solution of PCB (Printed Circuit Board) containing magnetic material, *IEEE Power electronics specialists conference,* 1998, Vol.2 D-6-5, pp1675-1680.
3. Saito, Y., Takahashi, K., Hayano, S., Finite element solution of unbounded magnetic field problem containing ferromagnetic materials, *IEEE Trans. Magn,* 1998, Vol.24, No.6, pp.2946-2948.
4. Takahashi, K., Saito, Y., Hayano, S., The strategic dual image method for the open boundary electromagnetic field problems, *Int. J. Appl. El. Mat.*, 1993, Vol.4, pp.178-184.